Distinguished Author Series

Interpretation of Tests in Fissured and Multilayered Reservoirs With Double-Porosity Behavior: Theory and Practice

by Alain C. Gringarten, SPE

Alain C. Gringarten is vice president of Scientific Software-Intercomp in Denver. He earlier was director of engineering with Johnston-Macco-Schlumberger in Houston and during 1978–81 head of well test interpretation with Flopetrol-Schlumberger in France. A graduate of Stanford U., Gringarten has published more than 30 papers on well test analysis and related subjects. He currently serves on the SPE Editorial Review Committee.

Summary

This paper summarizes current knowledge of reservoirs with double-porosity behavior. These include both naturally fissured reservoirs and multilayered reservoirs with high permeability contrast between layers. The first part presents available solutions to the direct problem (i.e., solutions to the diffusivity equation) that have appeared in the oil and groundwater literature over the past 20 years. The second part discusses methods for solving the inverse problem—i.e., identifying a double-porosity behavior and evaluating all corresponding well and reservoir parameters.

Several field examples demonstrate various aspects of double-porosity behavior and illustrate how additional knowledge of the reservoir (e.g., fissured vs. multilayered, gas saturation, etc.) can be obtained from numerical values of the reservoir parameters. Practical considerations for planning tests in double-porosity reservoirs also are included.

Introduction

The movement of underground fluids is of interest in many different engineering fields and, consequently, has been the subject of active research over the past 40 years.

Interpretation procedures, however, are well established only for porous fluid-bearing reservoirs considered reasonably homogeneous. Fluid-flow behavior in heterogeneous formations is still the subject of much debate. It is agreed only that conventional methods primarily developed for homogeneous reservoirs may be inadequate, and that new specific approaches may be required to provide a convincing explanation for some commonly observed flow peculiarities.

There has been no unified approach to the problem; heterogeneous reservoir behavior in the literature is still considered too complex and too diverse to be analyzed in a systematic and unique way. The main reason is the general belief that an interpretation model must closely approximate the actual complexity of the reservoir. The observation of a very large number of well tests in many different formations around the world, however, reveals that the number of possible behaviors during a well test is limited; therefore, only a limited number of interpretation models is required for well test analysis. This is because during a well test, the reservoir is acting only as a filter between an input signal, the change in flow rate, and an output signal, the change in pressure, and only high contrasts in physical properties within the reservoir can be highlighted.

In practice, a test reveals only that the reservoir acts as one single medium (homogeneous behavior) or as two interconnected media (heterogeneous behavior). The terms "homogeneous" and "heterogeneous" are related to reservoir behavior, not to reservoir geology. "Homogeneous" means that the permeability measured in a test and that measured in a core are the same, although the resulting numbers may be different. "Heterogeneous" means that these permeabilities are likely to be different.

The Double-Porosity Model

The particular case of heterogeneous behavior where only one of the two constitutive media can produce to the well is called "double-porosity" behavior.

0149-2136/84/0041-0044$00.25

Although the corresponding double-porosity model has been the subject of many studies in the past 20 years, its use is still not fully understood by the practicing engineer. This model is discussed in detail in the remainder of this paper.

The double-porosity model initially was introduced for the study of fissured reservoirs.[1-8] Later, several authors proposed the two-layered model as an alternative solution.[9,10] In reality, both fissured and multilayered reservoirs with high permeability contrast between layers can be represented by the same double-porosity model[11] and exhibit the same double-porosity behavior during a test. As a result, it is impossible to distinguish between the two types from pressure-test behavior alone. As discussed below, distinction can be made only under certain conditions from the numerical values of the well and reservoir parameters.

A detailed review of published articles on double porosity as applied to fissured reservoirs was presented in Ref. 11. The following summarizes only current knowledge of the double-porosity model. Solutions to the direct problem (i.e., predicting the pressure behavior of a double-porosity reservoir) are presented first, followed by a detailed discussion of the inverse problem (i.e., identifying a double-porosity reservoir from test data alone and evaluating double-porosity reservoir parameters). The latter is illustrated with field examples.

Direct Problem: Mathematical Models for Double-Porosity Behavior

The double-porosity concept was introduced by Barenblatt *et al.*[1] As mentioned before, the double-porosity model assumes the existence of two porous regions of distinctly different porosities and permeabilities within the formation. Only one of the porous media has a permeability high enough to produce to the well. This would be the fissure system in a fissured reservoir or the most permeable layer in a two-layered reservoir. For simplicity, I sometimes in the following call it "the fissures" and refer to it with the subscript f.

The second porous medium does not produce directly into the well but feeds fluid into the first medium and acts as a source. This would correspond to the matrix blocks in a fissured reservoir and to the less permeable layer in a two-layered reservoir. Again, for simplicity, I refer to it as "the blocks" and use the subscript m. The subscript $f+m$ stands for the total system.

A basic assumption in the model in Ref. 1 is that any infinitesimal volume contains a large proportion of each of the two constitutive media. As a consequence, each point in space is associated with two pressures, namely: (1) the average fluid pressure, p_f, in the most permeable medium in the vicinity of the point and (2) the average fluid pressure, p_m, in the least permeable medium in the vicinity of that same point. p_f is the pressure measured at the bottom of the well during a test.

A very important characteristic of a double-porosity system is the nature of the fluid exchange between the two constitutive media, or interporosity flow. Interporosity flow was assumed by Barenblatt *et al.*[1] and by subsequent authors[2,3,5,7,12] to occur under pseudosteady-state conditions:

$$\delta q=\alpha\frac{k_m}{\mu}(p_m-p_f), \quad \ldots\ldots\ldots\ldots\ldots\ldots\ldots\ldots\ldots\ldots (1)$$

where k_m is the permeability in the least permeable medium, α, a parameter characteristic of the geometry of the system, has the dimension of a reciprocal area:

$$\alpha=\frac{4n(n+2)}{\ell^2}, \quad \ldots\ldots\ldots\ldots\ldots\ldots\ldots\ldots\ldots\ldots (2)$$

where n is the number of normal sets of planes limiting the least permeable medium ($n=1$ for a multilayered reservoir) and ℓ is a characteristic dimension of such a block.

Other authors[6,8-10,13-15] have assumed transient interporosity flow. Among these, de Swaan[6] presented a particularly interesting approach used in several subsequent publications[8,13,14,17] (see Appendix).

The question of the interporosity flow condition likely to be found in practice has been the subject of much debate in the past few years. Pseudosteady state has been shown to be a long-time approximation of transient interporosity flow,[7] and the pseudosteady-state assumption has been justified because any transient effect was likely to be of short duration, as could be inferred from published formulas describing the initiation of pseudosteady-state flow.[16] Indeed, the majority of tests I have seen appear to exhibit a pseudosteady-state interporosity flow behavior. Yet some other tests seemed to indicate a transient interporosity flow behavior, which is distinctly different.[17]

A possible explanation of this apparent inconsistency can be found in an unpublished paper by Cinco,* who suggests that interporosity flow always occurs under transient conditions but can exhibit a pseudosteady-state-like behavior if there is significant impediment to the flow of fluid from the least permeable medium to the most permeable one, as in the case of calcite deposit in a fissured reservoir, for instance. In fact, interporosity flow can exhibit any intermediate behavior, depending upon the magnitude of the interporosity skin.

As occurred in the case of reservoirs with

*Cinco-Ley, H.: Personal communication (Oct. 28, 1983).

homogeneous behavior, the first solutions for double-porosity behavior were limited to line-source wells. Although Barenblatt *et al.*[1] introduced the double-porosity concept, they only derived the pressure in the blocks with the restriction of zero compressibility in the most permeable medium.

The first complete line-source solution in terms of pressure in the most permeable medium was done by Warren and Root[2] for pseudosteady interporosity flow. These authors showed that two parameters, in addition to permeability and skin, controlled double-porosity behavior. These are: (1) the ratio ω of the storativity in the most permeable medium to that of the total reservoir,

$$\omega=\frac{(\phi Vc_t)_f}{(\phi Vc_t)_{f+m}}, \quad \ldots\ldots\ldots\ldots\ldots\ldots\ldots\ldots\ldots\ldots (3)$$

where V is the ratio of the total volume of one medium to the bulk volume, and ϕ is the porosity of that medium (ratio of pore volume in the medium to the total medium volume); and (2) the interporosity flow coefficient λ,

$$\lambda=\alpha r_w^2\frac{km}{k_f}, \quad \ldots\ldots\ldots\ldots\ldots\ldots\ldots\ldots\ldots\ldots (4)$$

where k_f is the permeability of the most permeable medium.

Other line-source solutions subsequently published are essentially identical to that of Warren and Root,[3,5-7] or they consider transient interporosity flow.[7,14,15]

Wellbore storage and skin were added to the pseudosteady-state interporosity flow solution of Warren and Root by Mavor and Cinco.[12] This solution then was extended by Bourdet and Gringarten[17] to account for transient interporosity flow and to generate type curves useful for the analysis of double-porosity systems. A similar solution later was published by Cinco and Samaniego.[13]

Inverse Problem: Identification of Double-Porosity Behavior From Well-Test Data

Conventional Semilog Analysis. The first identification method was proposed by Warren and Root.[2] These authors evaluated approximate forms of their pseudosteady-state interporosity flow solution and found that they yielded two parallel straight lines on a semilog plot (Fig. 1). The first straight line represents homogeneous semilog radial flow in the most permeable medium acting alone, whereas the second straight line corresponds to semilog radial flow in the total reservoir. The two straight lines are separated by a transition period during which pressure tends to stabilize.

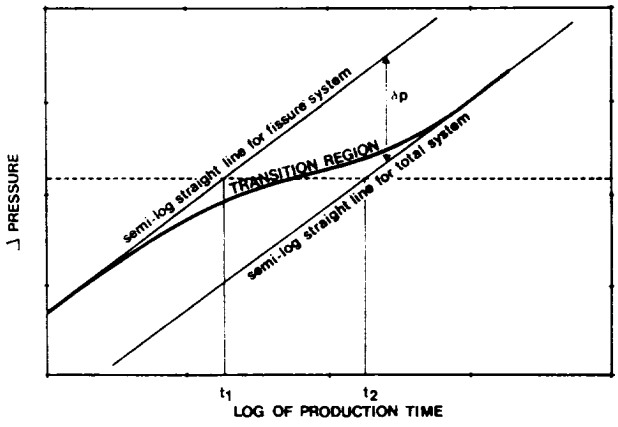

Fig. 1—Drawdown test in a double-porosity reservoir (Warren and Root[2]): two parallel semilog straight lines.

Conversely, as Warren and Root had derived their direct solution for fissured systems, they suggested that this two parallel semilog straight-line behavior was characteristic of fissured reservoirs. They noted, however, that it was also characteristic of stratified formations (i.e., it belongs to double-porosity behavior).

Warren and Root indicated that the reservoir permeability-thickness product, kh (in practice, the permeability-thickness product of the most permeable medium, k_fh, as the matrix blocks do not flow to the well), could be obtained from the slope m of the two semilog straight lines; ω, from their vertical displacement δp:

$$\omega=10^{-\delta p/m}; \quad \ldots\ldots\ldots\ldots\ldots\ldots\ldots\ldots\ldots\ldots (5)$$

and λ, from the time of intersection of the horizontal line drawn through the middle of the transition curve, with either the first (t_1) or the second (t_2) semilog straight line. This was shown by Bourdet and Gringarten[17] to yield

$$\lambda=\frac{(\phi Vc_t)_f\mu r_w^2}{\gamma k_f t_1}=\frac{(\phi Vc_t)_{f+m}\mu r_w^2}{\gamma k_f t_2} \quad \ldots\ldots\ldots\ldots (6)$$

in drawdown tests, and

$$\lambda=\frac{(\phi Vc_t)_f\mu r_w^2(t_p+\Delta t_1)}{\gamma k_f t_p\Delta t_1}=\frac{(\phi Vc_t)_{f+m}\mu r_w^2(t_p+\Delta t_2)}{\gamma k_f t_p\Delta t_2} \quad \ldots\ldots\ldots\ldots\ldots\ldots (7)$$

in buildup tests. t_p in Eq. 7 represents the duration of the drawdown preceding the buildup.

As t_1 and t_2 can only be approximated, the value of λ obtained by this method (and by others published in the literature[18]) is not very accurate but usually remains within the order of magnitude of the correct value. A more accurate method by type-curve analysis is discussed later.

The existence of the two parallel semilog straight lines, and therefore the possibility of obtaining ω and λ from test data, was disputed by Odeh,[3,19] who found that some fissured reservoirs could behave like homogeneous systems. Odeh investigated the same double-porosity model as Warren and Root but for different ranges of parameters.

In the case of transient interporosity flow, a third semilog straight line was shown to be present during transition,[17] with a slope equal to half that of the two parallel semilog straight lines.[13-15]

The conditions of the existence of the various semilog straight lines have been the subject of much discussion. It is generally believed that the first straight line, representing the most permeable medium, can exist only at very early times and is likely to be shadowed by wellbore storage effects. Therefore, a common perception is that, in practice, only parameters characterizing the homogeneous behavior of the total system, $k_f h$, can be obtained, as contended by Odeh[3]—assuming, of course, that the corresponding semilog straight line *is* present—and those specific to the fissures (ω,λ) are usually not accessible.

To minimize wellbore storage effects and thus avoid masking development of the first semilog straight line, several authors have advocated the use of a downhole shut-in tool.[2,20] This, however, can help only in multilayered reservoirs, not in fissured reservoirs. As discussed in another part of this paper, storage effects in fissured reservoirs include the effect of fissures intersecting the well and usually are one or two orders of magnitude greater than storage effects in the wellbore.

Type-Curve Analysis. An answer to the question of the existence of the various double-porosity semilog straight lines, and, more generally, a solution to the inverse problem in double-porosity reservoirs in the presence of wellbore storage and skin was presented recently by Bourdet and Gringarten.[17] They showed that double-porosity behavior is controlled by the independent variables (defined in Appendix) p_D, t_D/C_D, $C_D e^{2S}$, ω, and λe^{-2S}, and that it is possible to represent the behavior of a well with wellbore storage and skin in an infinite reservoir with double-porosity behavior, $p_D = f(t_D/C_D, C_D e^{2S}, \omega, \lambda e^{-2S})$, as a combination of the homogeneous behavior of each constitutive porous medium, with wellbore storage and skin at the well: $p_D = f_h(t_D/C_D, C_D e^{2S})$ (with C_D in $C_D e^{2S}$ based on the storativity of the medium under consideration), and behavior during interporosity flow from the least permeable medium into the most permeable one: $p_D = f_t(t_D/C_D, C_D e^{2S}, \lambda e^{-2S})$.

Bourdet and Gringarten[17] thus designed two drawdown type curves for a well with wellbore storage in an infinite reservoir with double-porosity behavior, corresponding to the two extreme interporosity flow conditions identified by Cinco,* namely, restricted and unrestricted interporosity flow. The former corresponds physically to a high skin between the most and the least permeable media and is mathematically equivalent to the pseudosteady-state interporosity flow solution. The latter corresponds to zero interporosity skin.

The type curve for restricted interporosity flow presented in Fig. 2 is obtained as the superposition of: (1) the drawdown type curve for a well with wellbore storage and skin in a reservoir with homogeneous behavior, presented in Ref. 21 (the continuous curves in Fig. 2), and (2) restricted interporosity flow curves, function of λe^{-2S} (the dashed lines in Fig. 2).[17]

The type curve for unrestricted interporosity flow presented in Fig. 3 is obtained as the superposition of: (1) the drawdown type curve for a well with wellbore storage and skin in a reservoir with homogeneous behavior, Ref. 21, and (2) unrestricted interporosity flow curves, function of $\delta[(C_D e^{2S})_{f+m}/\lambda e^{-2S}]$, shown as dashed lines in Fig. 3.[17] These transition curves are in fact the homogeneous curves of Ref. 21, shifted by a factor of 2. δ is a function of the shape of the matrix blocks and is given by: $\delta = 6/\gamma^2 = 1.89$ for horizontal slab matrix blocks, and $\delta = 10/3\gamma^2 = 1.05$ for spherical matrix blocks, where γ is the exponential of the Euler constant.

A typical behavior of the well pressure in a double-porosity reservoir is sketched in Fig. 4. At early times, production comes only from the most permeable medium, and the pressure drop follows one of the homogeneous curves with $C_D e^{2S} = (C_D e^{2S})_f$. This corresponds to the heavy line up to Point A on the curve called "fissures" on Fig. 4.

As interporosity flow starts from the least permeable medium into the most permeable one, the pressure leaves the $C_D e^{2S}$ curve and follows one of the transition curves (the heavy line between A and B on Fig. 4).

Finally, when all production comes from the least permeable medium, the pressure leaves the transition curve and follows a new $C_D e^{2S}$ curve below the first one, with $C_D e^{2S} = (C_D e^{2S})_{f+m}$, corresponding to homogeneous behavior of the total reservoir. This corresponds to the heavy line after Point B on the curve labeled "blocks + fissures" on Fig. 4.

Because the type curve for wellbore storage and skin

*Cinco-Ley, H.: Personal communication (Oct. 28, 1983).

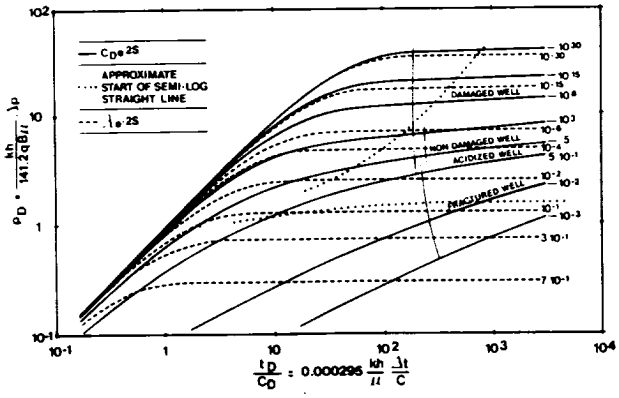

Fig. 2—Bourdet and Gringarten's type curve[17] for a well with wellbore storage and skin in a double-porosity reservoir (restricted interporosity flow).

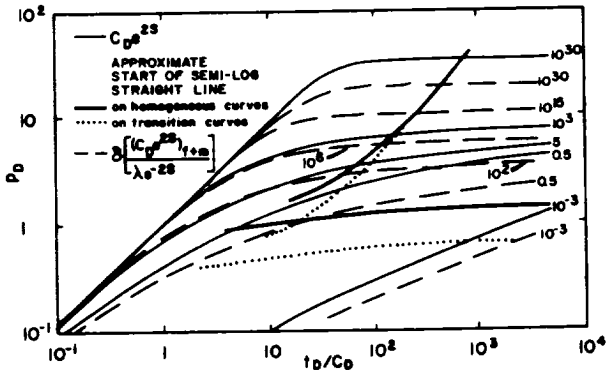

Fig. 3—Bourdet and Gringarten's type curve[17] for a well with wellbore storage and skin in a double-porosity reservoir (unrestricted interporosity flow).

in a reservoir with homogeneous behavior also includes the case of an infinite conductivity vertical fracture with wellbore storage (all continuous curves below $C_De^{2S} = 1$ in Figs. 2 and 3), the double-porosity type curves in Figs. 2 and 3 yield information on the quality of the well, depending on the C_De^{2S} curve matching the homogeneous behavior of the most permeable medium: *damaged* if $(C_De^{2S})_f$ is greater than 10^3; *normal* (nondamaged) if $(C_De^{2S})_f$ is between 10^3 and 10^5; *acidized* if $(C_De^{2S})_f$ is between 5 and 0.5; and *fractured* if $(C_De^{2S})_f$ is less than 0.5. These limits, of course, are only approximate.

The use of the double-porosity type curves is discussed in the remainder of this paper, to illustrate some characteristic features of double-porosity behavior. Most comments concern the type curve of Fig. 2, for the sake of simplicity and because, in my experience, restricted interporosity flow is the most common behavior found in practice. These comments and conclusions extend readily to unrestricted interporosity flow.

Drawdown Analysis. When the total system behavior is seen during a test, as in Fig. 4, log-log analysis of drawdown data with the type curves of Figs. 2 and 3 yields all the parameters normally obtained with the wellbore storage and skin type curve for homogeneous reservoirs,[21] namely: k_fh from the pressure match, C from the time match, and S from the match with the C_De^{2S} curve for which ϕVc_t is available (most permeable medium or total reservoir, usually the latter), plus the fissuration parameters: λ from the match with the transition curves λe^{-2S} or $\delta[(C_De^{2S})_{f+m}/\lambda e^{-2S}]$; ω from the ratio of the C_De^{2S} value for the last wellbore storage and skin homogeneous curve (corresponding to the total reservoir) to the C_De^{2S} value for the first wellbore

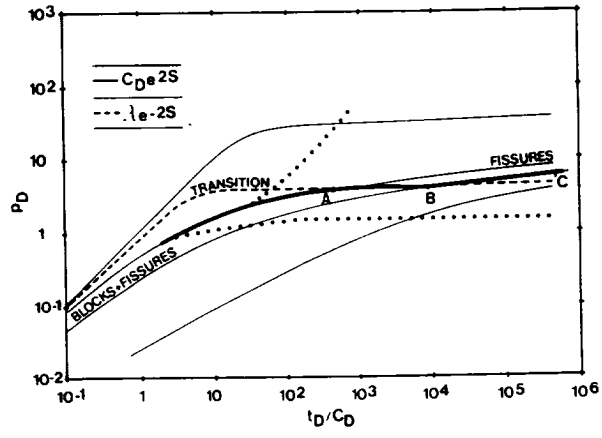

Fig. 4—Schematic of double-porosity log-log behavior.

storage and skin homogeneous curve (corresponding to the most permeable medium):

$$\omega = \frac{(C_De^{2S})_{f+m}}{(C_De^{2S})_f} \quad \ldots\ldots\ldots\ldots\ldots\ldots\ldots\ldots (8)$$

Occasionally, the first C_De^{2S} curve coincides with the transition curve so that the well drawdown pressure follows the transition curve from the very beginning before merging into a C_De^{2S} curve corresponding to the total reservoir. This situation occurs when $(\phi Vc_t)_f$ is very small compared to $(\phi Vc_t)_{f+m}$. The actual $(C_De^{2S})_f$ curve may in fact be to the left of the λe^{-2S} curve, and the actual $(C_De^{2S})_f$ value may be greater than that of the C_De^{2S} curve coinciding with the early part of the transition curve. Log-log analysis in such a

case still yields $k_f h$, C, S, and λ as before, but only an upper limit of ω:

$$\omega \leqslant \frac{(C_D e^{2S})_{f+m}}{(C_D e^{2S})_{f,\text{lim}}}. \quad \ldots\ldots\ldots\ldots\ldots\ldots\ldots\ldots (9)$$

In practice, it is difficult to detect ω values of less than 0.001 by type-curve analysis.

Of course, if only a portion of the complete double-porosity drawdown behavior shown in Fig. 4 is obtained during the test, only limited information can be extracted from the test data. For instance, it is not possible in practice to read λe^{-2S} values much greater than unity. In such a case, the most permeable medium behavior is not visible, and only the last $C_D e^{2S}$ curve, corresponding to homogeneous behavior of the total reservoir, can be obtained in the test. This may occur when the blocks in the least permeable medium are very small and the well is hydraulically fractured; the double-porosity reservoir then would behave like a homogeneous one, with the transmissivity of the most permeable medium, and the total storativity.

Similarly, the double-porosity nature of the reservoir may remain unnoticed if λe^{-2S} is small and the test not long enough, so that only the $C_D e^{2S}$ for the most permeable medium is recorded during the test (up to Point A in Fig. 4). In that case, analysis can only provide the same parameters as with homogeneous systems: $k_f h$, C, and S. The value for S would in fact be a maximum if the total storativity, instead of that of the most permeable medium, is used in the skin calculations.

Finally, another alternative behavior is seen when drawdown stops during transition. This case is examined in detail in connection with buildup analysis.

The type curves of Figs. 2 and 3 provide an explanation for the presence or the absence of the two parallel semilog straight lines described by Warren and Root[19] and of the semilog straight line during unrestricted interporosity transition flow.[13-15,17] Because the pressure drop in double-porosity behavior follows two homogeneous $C_D e^{2S}$ curves in Fig. 2 and three homogeneous $C_D e^{2S}$ curves in Fig. 3, respectively, two or three semilog straight lines *may* be present if conditions for semilog radial flow are satisfied on each $C_D e^{2S}$ curve.

In a drawdown test in a double-porosity reservoir with restricted interporosity flow, this requires matching each of the two $C_D e^{2S}$ drawdown curves in Fig. 2 beyond the dotted line, which indicates the approximate start of semilog radial flow. It is obvious from Fig. 2 that the occurrence of the two semilog straight lines requires a particular combination of $(C_D e^{2S})_f$, λe^{-2S}, and ω. It depends not only on the characteristics of the fluid and of the reservoir (λ and ω) but also and primarily on the well condition (S in $C_D e^{2S}$ and λe^{-2S}). This makes it difficult to predict the existence of the two semilog straight lines and, moreover, does not guarantee that the two semilog straight lines found in a test will be found again in subsequent tests, and vice versa. Of course, if the two semilog straight lines exist, they must be parallel, because the permeability thickness of the total system is equal to that of the most permeable medium.

In a drawdown test in a double-porosity reservoir with unrestricted interporosity flow, the additional half-slope semilog straight line exists for test data matching the transition curves in Fig. 3 after the dotted curves labeled "approximate start of semilog radial flow on transition curves."

In a buildup, conditions for the occurrence of the two parallel semilog straight lines on a Horner plot are: (1) the preceding drawdown must be long enough for total reservoir behavior to be reached—i.e., the last $C_D e^{2S}$ curve; (2) semilog radial flow must exist on the first $C_D e^{2S}$ curve before transition occurs; and (3) buildup time must be greater than the time required to reach semilog radial flow on the final $C_D e^{2S}$ drawdown type curve. The existence of the two parallel semilog straight lines on a Horner plot thus requires a drawdown of adequate duration in addition to the other conditions found for drawdown tests.

The duration of the drawdown is of primary importance for the analysis of buildup tests in double-porosity reservoirs and controls the number of parameters that can be extracted from test data. Its impact on buildup test analysis is examined in detail below.

Buildup analysis. In practice, drawdown data are difficult to analyze because they usually are perturbed by variations of flow rate. As a result, analysis is often made on buildup data only.

Analysis of buildup data in double-porosity reservoirs, however, is a lot more complicated than in homogeneous formations. The main reason is that, for log-log analysis, log-log buildup type curves are required; drawdown type curves are usually inadequate because drawdown and buildup durations are often of the same order, especially in exploration tests.

Buildup type curves for a well with wellbore storage and skin in a double-porosity reservoir can be constructed as the drawdown type curves of Figs. 2 and 3 by superposing buildup type curves for a well with wellbore storage and skin in a homogeneous reservoir with the transition curves. As a result, transition during buildup occurs at the same Δp level as in drawdown but at a later time, assuming, of course, that duration of drawdown is long enough for total reservoir behavior to be seen. If this is not the case, the problem becomes even more complicated.

Horner analysis is also more delicate than with homogeneous reservoirs and requires a lot of caution.

Fig. 5 illustrates several possibilities found in practice. Five buildup curves are shown on a Horner plot, each computed for a different drawdown duration. The corresponding log-log plots are presented in Figs. 6 through 10.

Fig. 6 presents an example of drawdown and buildup log-log plot when drawdown duration is long enough for the total system to be seen. This is the most desirable situation. All well and reservoir parameters can be extracted from drawdown data by log-log analysis. In the same way, log-log analysis of buildup data (Curve E in Fig. 6) with the corresponding buildup type curve will yield all the well and reservoir parameters ($k_f h$, C, S, ω, and λ) if the buildup test is long enough to reach the last $C_D e^{2S}$ buildup curve.

Horner analysis, on the contrary, will yield all the parameters only if the two parallel semilog straight lines exist (this is the case in the example selected for preparing Fig. 5). If only the last semilog straight line exists, only $k_f h$, S, and p^* can be obtained; i.e., the fissuration parameters ω and λ are accessible only through log-log analysis. In both cases, the intercept p^* of the second semilog straight line represents the reservoir initial pressure.

Another case of interest is presented in Fig. 7. Drawdown duration is such that only the most permeable medium is produced: drawdown pressure data remain on the first $C_D e^{2S}$ curve, the transition curve is not reached. As discussed before, the double-porosity nature of the reservoir cannot be diagnosed from drawdown data, nor from buildup data, either on a log-log or on a Horner plot (Curve A in Figs. 7 and 5, respectively).

Log-log analysis with the type curve for a well with wellbore storage and skin in a homogeneous reservoir[21] can yield all homogeneous reservoir parameters ($k_f h$, C, and S) from either drawdown or buildup data. S is only a *maximum* value if the total system storativity is used in the skin calculations, instead of that for the most permeable medium. If it is known that the reservoir is a double-porosity system (e.g., from tests in other wells), a *maximum* value for λ can be obtained by using the λe^{-2S} transition curve crossing the drawdown $C_D e^{2S}$ curve for the most permeable medium at a t_D/C_D value corresponding to the dimensionless production time. ω cannot be evaluated.

Horner analysis is possible only if semilog radial flow exists on the first $C_D e^{2S}$ curve for the most permeable medium. If this is the case, as for Curve A in Fig. 5, it is possible to obtain $k_f h$, S, and p^*. Again, S is only a maximum; p^* represents the reservoir initial pressure.

The examples shown in Figs. 8 through 10 all correspond to drawdowns terminated during transition.

In Fig. 8, the drawdown stops after transition has

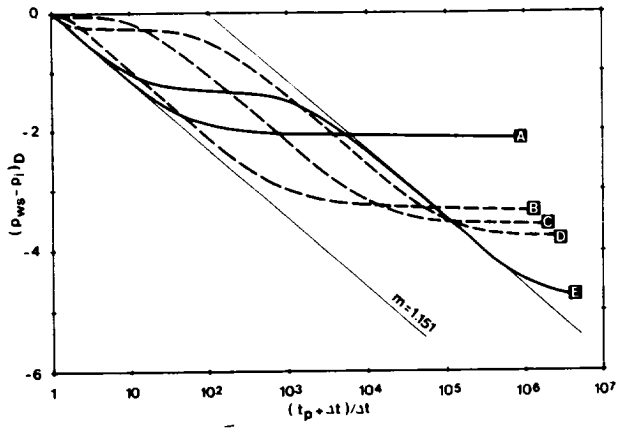

Fig. 5—Typical double-porosity behaviors on a Horner plot.

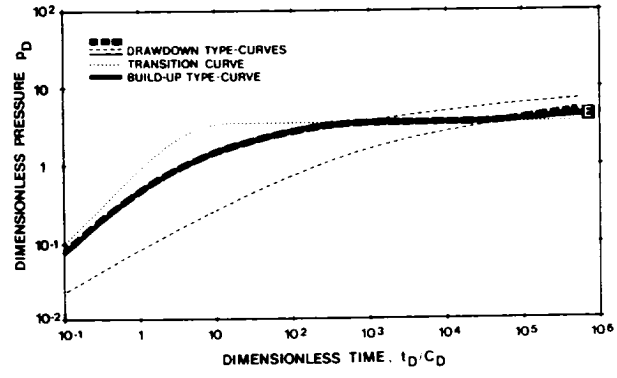

Fig. 6—Double-porosity buildup log-log behavior when total system is produced during drawdown.

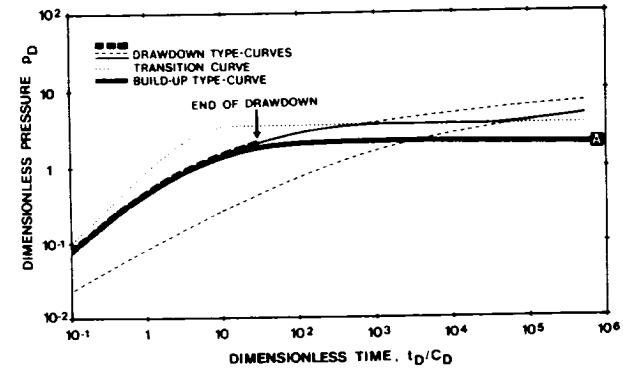

Fig. 7—Double-porosity buildup log-log behavior when only the most permeable medium is produced during drawdown.

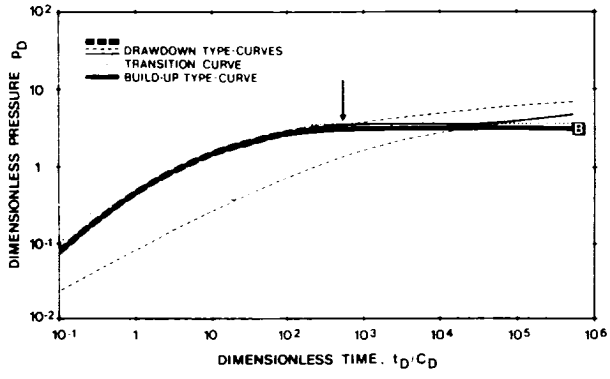

Fig. 8—Double-porosity buildup log-log behavior when drawdown stops in transition.

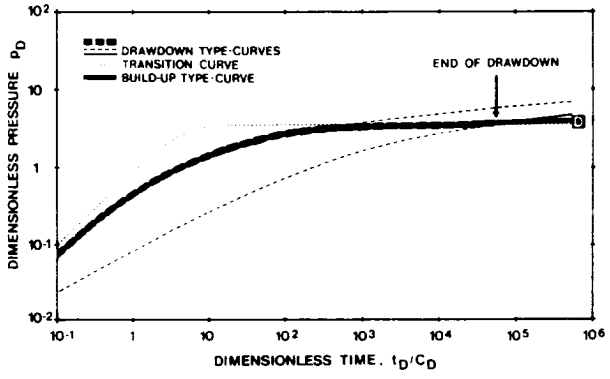

Fig. 10—Double-porosity buildup log-log behavior when drawdown stops in transition.

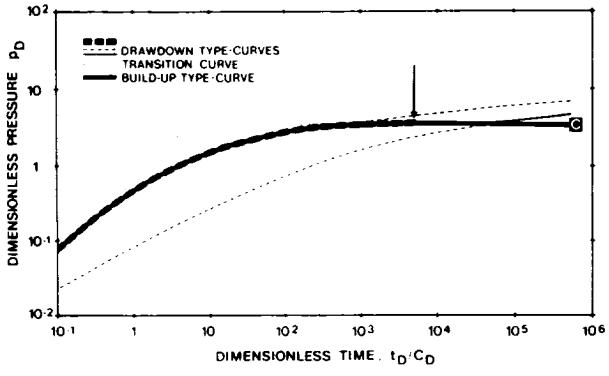

Fig. 9—Double-porosity buildup log-log behavior when drawdown stops in transition.

started but before the stabilized transition pressure, corresponding to the λe^{-2S} curve, has been reached. The corresponding buildup (Curve B in Fig. 8) starts on the buildup curve for the most permeable medium and then flattens out like a constant pressure boundary. The total reservoir $C_D e^{2S}$ curve is not seen in practice whatever the buildup duration.

As the constant pressure portion on the log-log occurs below the level of the λe^{-2S} curve, a maximum value of λe^{-2S} can be obtained by fitting a λe^{-2S} transition curve through these points. As with curve A discussed above, log-log analysis yields $k_f h$, C, and maximum values of S and λ.

On the Horner plot, the constant pressure portion gives a minimum value for the reservoir average pressure (Curve B in Fig. 5). If the buildup is too short for this constant pressure effect to be seen, the buildup curve on the Horner plot is very similar to the Curve A discussed before. The difference lies in the fact that the final semilog straight line, indicated by the label $m=1.151$ in Fig. 5, is not reached. There is another straight line, however, with a slope almost equal (at least in the example discussed) that could be mistaken for the Horner semilog straight line. If used for Horner analysis, this "wrong" straight line may yield a $k_f h$ close to the actual one, but a wrong value of the skin and of p^*. If p^* is taken to represent the reservoir pressure, signs of depletion could be found erroneously by comparison with other tests with different drawdown durations.

In Fig. 9, the drawdown stops in the middle of the transition period on the λe^{-2S} curve. This case is very similar to that of Fig. 8 except that the constant pressure portion during the buildup (Curve C) coincides with the transition curve on the log-log match.

As for the preceding case, log-log analysis yields $k_f h$, C, a maximum value for S (if total storativity is used), and a maximum value for λ. In addition, a *maximum* value for ω can be obtained from the buildup $C_D e^{2S}$ type curve passing through the last buildup point.

Horner analysis (Curve C in Fig. 5) is similar to that with Curve B. In this case, however, the constant pressure portion usually is well defined, thus giving a minimum value of the reservoir average pressure, $\bar{p}$. If semilog radial flow is seen in the most permeable medium (the "first" semilog straight line), a maximum value of ω can be obtained from Eq. 5, with $\delta p = \bar{p} - p^*_f$, p^*_f being the intercept of the "first" semilog straight line. In most practical cases, the buildup is not long enough to see the total system behavior. Even if it is long enough, the "second" semilog straight line is not well defined.

Finally, in Fig. 10 the drawdown stops just before reaching the total system curve. On the buildup type curve (Curve D in Fig. 10), the pressure tends to stabilize just above the λe^{-2S} curve, so a *minimum*

value of λe^{-2S} can be found, in theory, by fitting a transition curve through the constant pressure points. In nondamaged or stimulated wells, it may even be possible to find a unique combination of ω and λe^{-2S} if distinct evidence of the total reservoir behavior can be seen in the buildup data. As before, $k_f h$, C, and a maximum value of S are obtained from log-log analysis if the total storativity is used.

From the Horner plot, the buildup appears like a constant pressure boundary effect in nearly all practical cases (Curve D in Fig. 5). However, if the buildup is very long, the shape on the Horner plot is more characteristic of double-porosity behavior but the "second" semilog straight line may not be well-defined. A minimum value of average reservoir pressure and a maximum value of ω can be obtained as described before.

Analysis With Pressure Derivatives. From the description of the various features of a double-porosity reservoir, it is evident many of the behaviors described in this paper can be analyzed by using a *homogeneous model with appropriate boundary conditions.* This is obvious for the cases illustrated in Figs. 5, 9, and 10 with Curves C and D, when drawdown stops during transition. Curves C and D could be analyzed in terms of a homogeneous reservoir with a constant pressure boundary or in terms of a closed homogeneous reservoir. In the same way, the last $C_D e^{2S}$ curve in Fig. 4, corresponding to total reservoir behavior, could be mistaken for a sealing fault in a homogeneous reservoir.

Thus, there is often an alternative to the double-porosity model that uses the homogeneous model and attributes to boundary effects the features that characterize double-porosity behavior. Fortunately, the results of such an interpretation are often questionable, distances to boundaries are often ridiculous (usually less than 100 ft [30 m]), and reservoir sizes are incredibly small (often less than 40,000 sq ft [3716 m^3]). Moreover, as discussed later, values for C and S may suggest a fissured reservoir even if the analysis has been performed with the homogeneous model.

In some cases, results from interpretation with the homogeneous model appear reasonable. In such a case, no choice can be made without additional information.

The homogeneous model has been used extensively and is still used for the analysis of fissured reservoirs.[11] In fact, it was the only real tool available before knowledge of the double-porosity model reached the state described in this paper. Among the various possibilities, the homogeneous model with a uniform-flux vertical fracture is certainly the most popular. It had been found[22,23] to describe reasonably well the behavior of wells intersecting natural fractures and often has been used to analyze tests in fissured formations. I now think that the homogeneous model with a uniform-flux fracture, or any other boundary condition, is not adequate for describing fissured reservoirs. As a matter of fact, a number of tests initially interpreted with the uniform-flux fracture have been reinterpreted with the double-porosity model. Results were found to provide a much more realistic description of the reservoir, as supported by other knowledge, than that obtained with the homogeneous model with a uniform flux fracture.

An efficient way to distinguish between homogeneous and heterogeneous behavior is to examine on a log-log plot the derivative of Δp with respect to the natural log of Δt, in the case of a drawdown, or with respect to the natural log of $\Delta t/(t_p + \Delta t)$ in the case of a buildup, as a function of Δt. Such a plot is characterized by a stabilization during semilog radial flow. The shape of the derivative for each behavior is drastically different,[24,25] with double-porosity behavior exhibiting a characteristic hump *below* the semilog radial flow stabilization level during transition, that allows unambiguous identification of the behavior, provided the quality of pressure data is adequate (Fig. 11). The pressure derivative also allows easy differentiation between an infinite reservoir with double-porosity behavior and a bounded reservoir with homogeneous behavior (whose Δp vs. Δt traces are superposed in Fig. 12, although they correspond to very different kh values). In the latter case, effects of boundaries appear *above* the semilog radial flow stabilization level, with a stabilization at twice that level for a sealing fault.

Field Examples

The following presents several field examples to illustrate the various double-porosity behaviors described in the first part of this paper. These examples have been selected from many tests with double-porosity behavior that I have seen and are fairly typical of what is found in practice.

Such examples are scarce in the literature.[2,3,11,20,26] One main reason is that most authors were trying to illustrate the two parallel semilog straight line feature, which is the exception rather than the rule. The following examples are used to introduce new information that cannot be derived from the theoretical developments presented so far but have been discovered through experience.

Fissured vs. Multilayered Reservoirs. It was stated in the beginning of this paper that the double-porosity model represents the behavior of both fissured and multilayered reservoirs with high permeability contrast between the layers. As a result, it is not possible, from the shape of the pressure vs. time curve alone, to distinguish between the two possibilities. All that can be diagnosed is a *double-porosity* behavior.

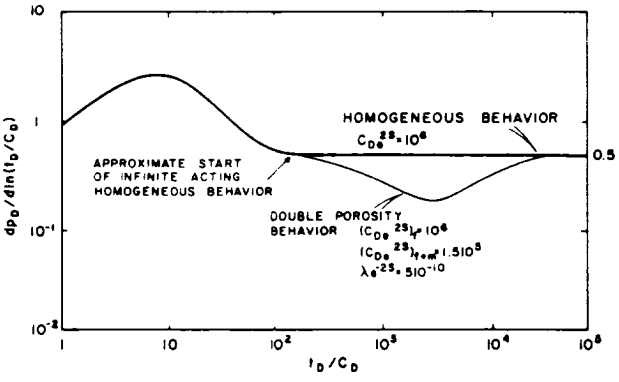

Fig. 11—Derivatives for homogeneous and double-porosity behavior.

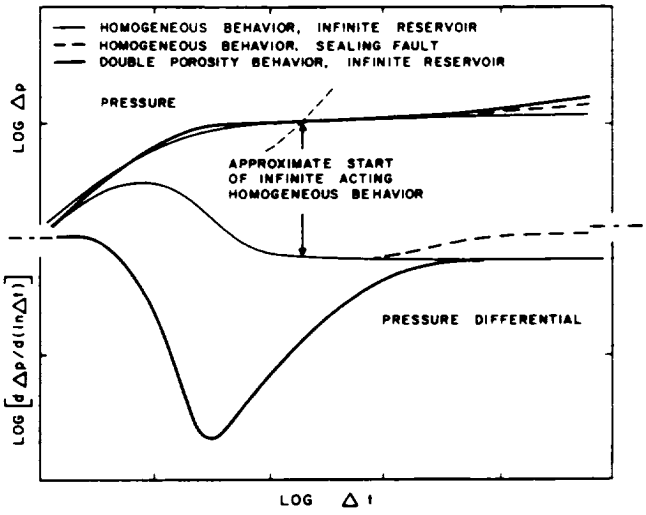

Fig. 12—Derivatives for homogeneous behavior in a bounded reservoir and double-porosity behavior in an infinite reservoir.

Fortunately, experience shows that this distinction is possible from the numerical values of the wellbore storage constant C and of the skin S if the well is not damaged. This is illustrated in Figs. 13 and 14, and in Table 1.

Figs. 13 and 14 present two examples of tests in double-porosity reservoirs, performed before and after an acid job. The details of the analyses are not shown, only the final log-log matches with the double-porosity type curve of Fig. 2. For each match, we have shown as a heavy line the double-porosity buildup (or drawdown, as appropriate) type curve fitted through the measured pressure points; the initial and final C_De^{2S} curves, corresponding to the most permeable and the least permeable medium, respectively, are indicated as dashed lines, and the λe^{-2S} transition curves are shown as dotted lines. For clarity, the type curves of Fig. 8 are not shown, only those limiting the various zones (damaged, nondamaged, acidized, and fractured wells).

Fig. 13 corresponds to unpublished buildup data from Well 1, whereas Fig. 14 presents drawdown data before acid and buildup data after acid from Test A in Well 2, whose analysis was presented in Ref. 26.

From the plots in Figs. 13 and 14 there appears to be no significant difference between the two series of tests from Wells 1 and 2, except that they match different double-porosity type curves. However, differences become apparent when one considers the numerical values of the parameters shown in Table 1.

Because all the flow components could be identified for Well 1 (initial and final C_De^{2S} curve and transition λe^{-2S} curve), it was possible to extract all the well and reservoir parameters pertinent to the double porosity model from the test data (i.e., k_fh, C, S, ω, and λ). On the other hand, the initial C_De^{2S} curve, representing the most permeable medium, could not be determined for Well 2 from the test before acid, due to lack of early-time data, and was found to coincide with the transition curve in the test after acid. As a result, ω could not be found before acid, and only an upper limit was found from post-acid data.

Let us now compare results before and after acid for each well. In Well 1 there is no variation in k_fh, as should be expected, nor in ω and λ. C has increased from 0.016 bbl/psi to 0.025 bbl/psi; this 50% increase could be attributed to the acid job. The skin has decreased from +3.4 to −3.9, which indicates a successful stimulation.

In Well 2, on the other hand, k_fh has decreased (but the pre-acid value is only approximate) while λ remains the same. But C has increased by almost *one order of magnitude*, from 0.017 bbl/psi to 0.13 bbl/psi. Skin has decreased from +3.4 to −1.5.

The increase in C after an acid job and the resulting high value of the wellbore storage constant are characteristic of fissured formations. Prior to the acid job, when the well is damaged, most of the fissures intersecting the wellbore are plugged and the volume of the fluid communicating with the wellbore is just the wellbore volume. The wellbore constant is thus equal to the one that could be computed from completion data if a value of fluid compressibility in the wellbore is available.

After the acid job, on the other hand, fissures become open to the wellbore and the volume of the fluid in direct communication with the well is equal to the wellbore volume plus the volume of the fissures intersecting the well. The resulting wellbore storage constant may be one or two orders of magnitude higher than before acid.

For this reason, downhole shut-in is not particularly

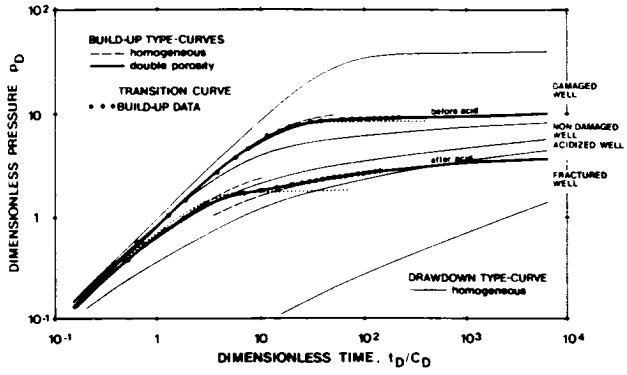

Fig. 13—Well 1 type-curve match for test before and after acid in a multilayered reservoir.

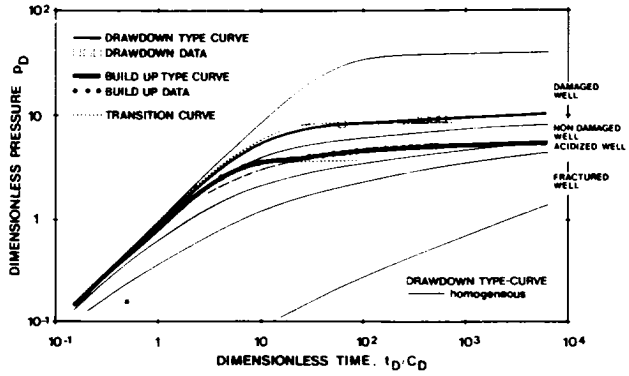

Fig. 14—Well 2 type-curve match for Test A before and after acid in a fissured reservoir.

TABLE 1—COMPARISONS BETWEEN INTERPRETATION RESULTS FROM WELL 1 AND WELL 2 (TEST A)

	Well 1 (Multilayered Reservoir)		Well 2, Test A (Fissured Reservoir)	
	Before Acid	After Acid	Before Acid	After Acid
$k_f h$, md-ft	565	565	416,600	347,000
C, bbl/psi	0.016	0.025	0.017	0.13
S	+3.4	−3.9	+3.4	−1.5
ω	0.10	0.10	?	$\leqslant 0.06$
λ	0.97×10^{-5}	1.0×10^{-5}	3.6×10^{-5}	3.6×10^{-5}

useful in fissured formations, except maybe with damaged wells.

On the other hand, there is no significant change in the wellbore storage constant following an acid job in a multilayered reservoir. As a result, fissured reservoirs can be distinguished from multilayered reservoirs with high permeability contrast between layers by means of the numerical value of the wellbore storage constant, but only if the well is not damaged. No distinction is possible from pressure and rate data alone if the well is damaged.

In this case, it can be concluded that Well 1 is in a multilayered reservoir, whereas Well 2 is in a fissured formation. These conclusions are supported by information from other sources.

Skin Value for Nondamaged Wells. Another interesting property of double-porosity reservoirs (whether fissured or multilayered) is illustrated by the examples in Figs. 13 and 14. Notice that for both wells, the initial $C_D e^{2S}$ curves, corresponding to the fissure system in Well 2 and to the most permeable layer in Well 1, lie, after acid, in the nondamaged well region of the type curves, not in the acidized well region, as should be expected. For Well 2 (Fig. 14), it is even at the limit between the regions for damaged and nondamaged wells. Yet skins are negative: −3.9 for Well 1 and −1.5 for Well 2.

In reality, double-porosity reservoirs exhibit pseudoskins, as created by hydraulic fractures. It is my experience that a skin of around −3 is normal for nondamaged wells in formations with double-porosity behavior. Acidized wells may have skins as low as −7, whereas a zero skin usually indicates a damaged well.

In the case of Well 2, the skin (−1.5 after acid) would indicate that the well is still damaged; as a result, some of the fissures communicating with the well may still be plugged, and C could increase further if a new acid job were performed.

Nondamaged or acidized wells in double-porosity formations thus are characterized by a very negative skin. This is associated with a high wellbore-storage constant in fissured reservoirs. Conversely, a very high wellbore-storage constant and a very negative skin should suggest a fissured reservoir, even if the well exhibits a homogeneous behavior. In general, this occurs when the test is too short, so that only the first $C_D e^{2S}$ curve corresponding to the fissures is seen in the test data. An example follows.

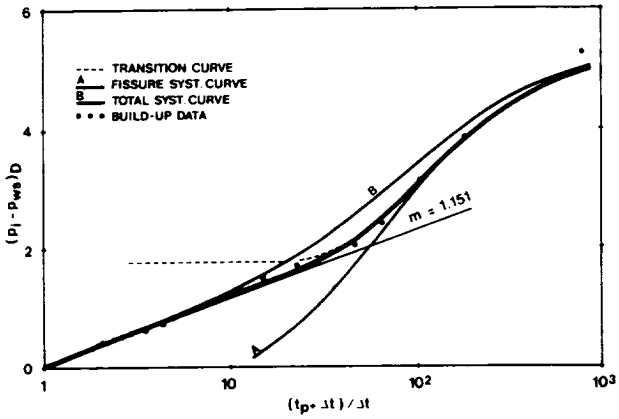

Fig. 15—Well 2 dimensionless Horner plot for Test A after acid.

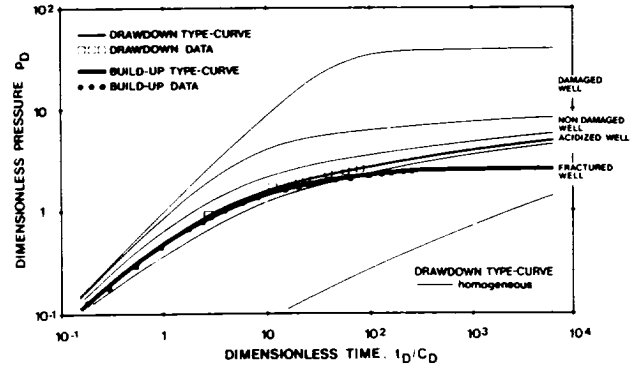

Fig. 16—Well 3 type-curve match for drawdown and buildup data.

Effect of Production Time on Buildup Behavior. This section illustrates the various buildup behaviors described earlier in the text.

The two tests in Fig. 13 for Well 1 and the test after acid in Fig. 14 for Well 2 are examples of buildup tests where the total system is seen in the test data. For these tests, the duration of the drawdown was sufficient for the total system to be present in drawdown data, but these were not adequate for analysis because of fluctuations in the flow rates.

As indicated in Table 1, it is possible to extract all the parameters pertinent to the double-porosity model from the test data.

Fig. 15 illustrates the Horner plot for the test after acid in Well 2. This corresponds to Curve E in Fig. 5, except that there is no "initial" semilog straight line. All the various flow components are indicated in Fig. 15: the first C_De^{2S} curve (A), the total system C_De^{2S} curve (B), and the transition curve. The "second" semilog straight line is reached by the buildup data.

TABLE 2—COMPARISON BETWEEN INTERPRETATION RESULTS FROM WELL 2 (TEST A), WELL 3, AND WELL 4

	Well 2 Test A After Acid	Well 3 After Acid	Well 4
k_fh, md-ft	347,000	2,260	90
C, bbl/psi	0.13	0.19	2×10^{-3}
S	−1.5	−5.1	−4
ω	$\leqslant 0.06$	?	?
λ	3.6×10^{-5}	?	2.5×10^{-6}

Fig. 16 presents drawdown and buildup data for Well 3 of Ref. 26, corresponding to Curve A of Figs. 5 and 7. This is the case where drawdown stops on the first C_De^{2S} curve before transition is reached. As a result, the data exhibit a homogeneous behavior and there is no evidence of a heterogeneous system except from the value of the parameters listed in Table 2: C (0.19 bbl/psi) is very large and the skin (−5.1) very negative, thus suggesting a fissured reservoir. In fact, some other wells in the same reservoir were found to exhibit a double-porosity behavior. Consequently, S is only a maximum value, since total storativity was used in the computations and a maximum value for λ can be computed ($\lambda \leqslant 3\times10^{-7}$).

The third example (Well 4 in Fig. 17) corresponds to the case where drawdown was stopped during transition. As a result, buildup pressure in Fig. 17 becomes stabilized at long buildup times. Analysis was performed as described earlier to yield k_fh, C, a maximum value for S, and a maximum value for λ. A maximum value for ω could not be evaluated because of insufficient data at constant pressure (see the Horner plot on Fig. 18). This case corresponds to Curve B in Figs. 5 and 8, where drawdown stops after transition has started but before the stabilized transition pressure, corresponding to the λe^{-2S} curve, has been reached.

Table 3 summarizes interpretation results for Well 2 (Fig. 14), Well 3 (Fig. 16), and Well 4 (Fig. 17). It shows clearly the dependency of results on the duration of drawdown: all reservoir parameters can be obtained only if both drawdown and buildup are long enough for total system behavior to be seen in the test data.

Variation of ω and λ With Time. Discussion so far has been based on the assumption that ω and λ were constant. This is not always the case, especially when reservoir pressure falls below bubble-point pressure. The reason is that ω and λ both depend on fluid properties, not just on rock characteristics. ω from Eq.

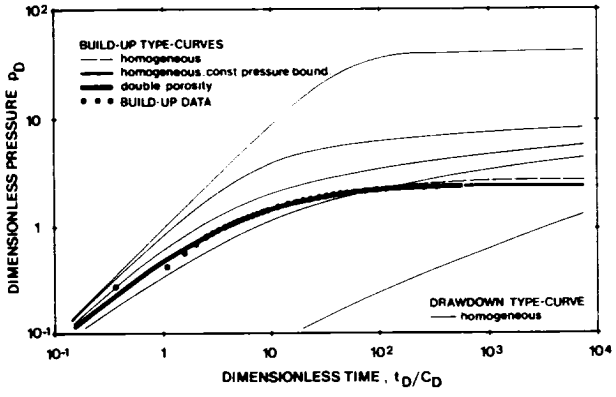

Fig. 17—Well 4 type-curve match of buildup data when drawdown stops in transition.

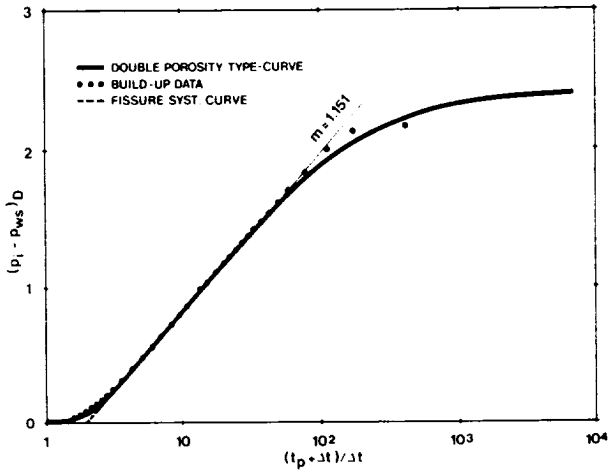

Fig. 18—Well 4 dimensionless Horner plot when drawdown stops in transition.

3 also can be written as:

$$\omega = \frac{1}{1 + \frac{(\phi V)_m}{(\phi V)_f}\frac{(c_t)_m}{(c_t)_f}}, \quad \ldots\ldots\ldots\ldots\ldots\ldots (10)$$

which clearly shows that ω depends on the ratio of the total compressibilities in both constitutive media. In the same way, λ depends on k_m, which is very sensitive to gas saturation.

An example illustrating changes in ω and λ in the same well is presented in Fig. 19. Data in Fig. 19 come from Test B in the same Well 2 used for Figs. 14 and 15. Tests A and B in Well 2 are discussed in detail in Ref. 26.

As can be seen by comparing Fig. 19 with Fig. 14, the buildup log-log behavior of Well 2 has changed drastically between Test A and Test B. The data in Test B exhibit a two parallel semilog straight-line behavior, evident on the Horner plot of Fig. 20, whereas in Test A, only the last semilog straight line was present (Fig. 15). The first semilog straight line in Fig. 20 lasts 14 hours. This change is attributed to the presence of gas in the reservoir. Complete analysis of the data was performed in Ref. 26 and results are listed in Table 3. It was possible to obtain not only $k_f h$, C, S, ω, and λ from both tests but also, using additional information to find the size of the matrix blocks, the change in total compressibility in the fissures and in the blocks and the change in matrix permeability from which the gas saturation in the blocks could be evaluated. Note that the well has become damaged, as evidenced from the increase in skin and the significant decrease in wellbore storage.

Variations of ω and λ with time usually indicate a change in the fluid characteristics. No change may also provide additional reservoir information. For example, no change in ω and λ after reservoir pressure has dropped below the bubble-point pressure would indicate that gas saturation is uniform in the reservoir. Testing at regular intervals is therefore advisable in reservoirs with double-porosity behavior.

TABLE 3—COMPARISON BETWEEN INTERPRETATION RESULTS FROM TEST A (AFTER ACID) AND TEST B IN WELL 2

	Well 2 Test A After Acid	Well 2 Test B After Acid
$k_f h$, md-ft	347,000	264,000
C, bbl/psi	0.13	0.03
S	−1.5	≥ -0.7
ω	≤ 0.06	0.43
λ	3.6×10^{-5}	$\geq 1.9 \times 10^{-6}$
c_{tm}	1	3
c_{tf}	1	36
k_m	1	1/21

Summary and Conclusions

The ambition of this paper is to establish the state of the art in the knowledge of double-porosity behavior. The information presented can be summarized as follows.

1. Fissured reservoirs and multilayered reservoirs with high permeability contrast between layers exhibit the same double-porosity behavior.
2. Double-porosity behavior can be diagnosed by log-log analysis of the pressure change during a test or by its derivative.

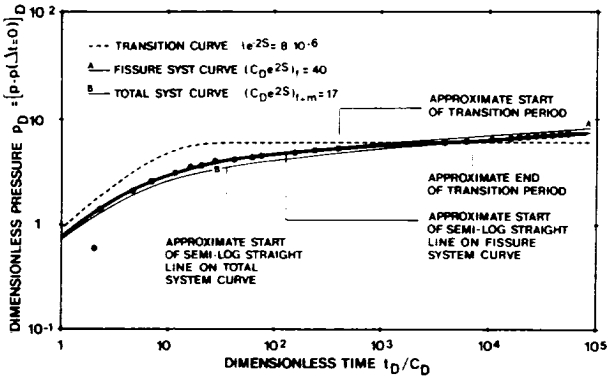

Fig. 19—Well 2 type-curve match for Test B with reservoir pressure below bubble-point pressure.

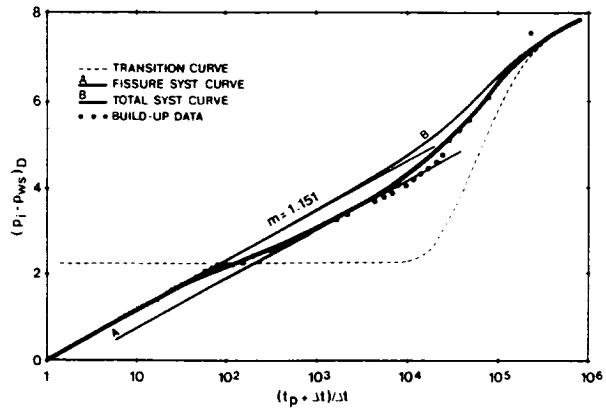

Fig. 20—Well 2 dimensionless Horner plot for Test B.

3. Analysis of tests in reservoirs with a double-porosity behavior using the double-porosity type curve of Figs. 2 and 3 can provide all pertinent reservoir parameters ($k_f h$, C, S, ω, and λ), even if these are not accessible by semilog analysis, on the condition that drawdowns and buildups are long enough to reach total system behavior. In most cases, however, matching must be done with buildup type curves. Once ω and λ are obtained, the total compressibility in the most permeable medium and dimensions of the least permeable medium can be computed if additional information is available, such as the geometry, total compressibility, and permeability of the least permeable medium.

4. The two parallel semilog straight-line feature may or may not exist, depending on the well condition and characteristics of each medium. When it does exist, the first semilog straight line may last for many hours.

5. Nondamaged wells in a double porosity exhibit a pseudoskin of around -3. Acidized wells can have skins as low as -7, whereas a zero skin usually indicates a damaged well.

6. Fissured reservoirs can be distinguished from multilayered reservoirs only if the well is nondamaged or acidized.

7. In multilayered reservoirs, the wellbore storage constant corresponds to the volume of the wellbore, whatever the well condition. On the contrary, nondamaged or acidized wells in fissured reservoirs exhibit a very high wellbore-storage constant that includes the volume of fissures intersecting the well. This wellbore storage is usually one or two orders of magnitude higher than that due to completion alone. As a result, downhole shut-in tools are ineffective in such wells. Wellbore storage in damaged wells in fissured reservoirs is normal—i.e., corresponds to the wellbore volume. Conversely, a negative skin associated with a high wellbore storage usually indicates a fissured reservoir even if the pressure behavior appears homogeneous. This may occur when the test is too short, so that only the fissure homogeneous behavior can be seen. A longer test is required to extract all the additional information (ω and λ) needed to describe the reservoir fully.

8. ω and λ may change with time for the same well depending on the characteristics of the reservoir fluid. Testing at regular intervals is recommended to obtain the information associated with such changes.

9. If the drawdown stops during transition, buildup behavior in double-porosity reservoirs is similar to that in homogeneous reservoirs with a boundary.

10. Interpreting heterogeneous reservoirs in terms of "equivalent" homogeneous reservoirs with inner or outer boundaries appears inadequate.

References

1. Barenblatt, G.E., Zheltov, I.P., and Kochina, I.N.: "Basic Concepts in the Theory of Homogeneous Liquids in Fissured Rocks," *J. Appl. Math. Mech.* **24**, 5 (1960) 1286–1303.
2. Warren, J.E. and Root, P.J.: "Behavior of Naturally Fractured Reservoirs," *Soc. Pet. Eng. J.* (Sept. 1963) 245–55; *Trans.*, AIME, **228**.
3. Odeh, A.S.: "Unsteady-State Behavior of Naturally Fractured Reservoirs," *Soc. Pet. Eng. J.* (March 1965) 60–66; *Trans.*, AIME, **234**.
4. Romm, E.S.: "Filtrasionnie Svoistsa Teschinovatich Porod (Flow Phenomena in Fractured Rocks)," Nedra, Moscow, in Russian (1966).
5. Kazemi, H., Seth, M.S., and Thomas, G.W.: "The Interpretation of Interference Tests in Naturally Fractured Reservoirs With Uniform Fracture Distribution," *Soc. Pet. Eng. J.* (Dec. 1969) 463–72; *Trans.*, AIME, **246**.
6. de Swaan O., A.: "Analytical Solutions for Determining Naturally Fractured Reservoir Properties by Well Testing," *Soc. Pet. Eng. J.* (June 1976).
7. Streltsova, T.D.: "Hydrodynamics of Groundwater Flow in a Fractured Formation," *Water Resources Res.* (1976) **12**, 3, 405–14.
8. Najurieta, H.L.: "A Theory for Pressure Transient Analysis in

Naturally Fractured Reservoirs," *J. Pet. Tech.* (July 1980) 1241-50.
9. Kazemi, H.: "Pressure Transient Analysis of Naturally Fractured Reservoirs With Uniform Fracture Distribution," *Soc. Pet. Eng. J.* (Dec. 1969) 451-62; *Trans.*, AIME, **246**.
10. Boulton, N.S. and Streltsova, T.D.: "Unsteady Flow to a Pumped Well in a Fissured Water-Bearing Formation," *J. Hydrol.* (1977) **35**, 257-69.
11. Gringarten, A.C.: "Flow Test Evaluation of Fractured Reservoirs," paper presented at the Symposium on Recent Trends in Hydrology, Geological Soc. of America, Berkeley, CA, Feb. 8-9, 1979.
12. Mavor, M.J. and Cinco, H.: "Transient Pressure Behavior of Naturally Fractured Reservoirs," paper SPE 7977 presented at the 1979 SPE California Regional Meeting, Ventura, April 18-20.
13. Cinco-L., H. and Samaniego-V., F.: "Pressure Transient Analysis for Naturally Fractured Reservoirs," paper SPE 11026 presented at the 1982 SPE Annual Technical Conference and Exhibition, New Orleans, Sept. 26-29.
14. Serra, K., Reynolds, A.C., and Raghavan, R.: "New Pressure Transient Analysis Methods for Naturally Fractured Reservoirs," *J. Pet. Tech.* (Dec. 1983) 2271-83.
15. Streltsova, T.D.: "Well Pressure Behavior of a Naturally Fractured Reservoir," *Soc. Pet. Eng. J.* (Oct. 1983) 769-80.
16. Muskat, M.: *The Flow of Homogeneous Fluids Through Porous Media*, J.W. Edward Inc., Ann Arbor, MI (1946).
17. Bourdet, D. and Gringarten, A.C.: "Determination of Fissured Volume and Block Size in Fractured Reservoirs by Type-Curve Analysis," paper SPE 9293 presented at the 1980 SPE Annual Technical Conference and Exhibition, Dallas, Sept. 21-24.
18. Uldrich, D.O. and Ershaghi, I.: "A Method for Estimating the Interporosity Flow Parameter in Naturally Fractured Reservoirs," *Soc. Pet. Eng. J.* (Oct. 1979) 324-32.
19. Warren, J.E. and Root, P.J.: "Discussion of Unsteady-State Behavior of Naturally Fractured Reservoirs," *Soc. Pet. Eng. J.* (March 1965) 64-65; *Trans.*, AIME, **234**.
20. Crawford, G.E., Hagedorn, A.R., and Pierce, A.E.: "Analysis of Pressure Buildup Tests in a Naturally Fractured Reservoir," *J. Pet. Tech.* (Nov. 1976) 1295-1300.
21. Gringarten, A.C. *et al.*: "A Comparison Between Different Skin and Wellbore Storage Type Curves for Early-Time Transient Analysis," paper SPE 8205 presented at the 1979 SPE Annual Technical Conference and Exhibition, Las Vegas, Sept. 23-26.
22. Gringarten, A.C., Ramey, H.J. Jr., and Raghavan, R.: "Unsteady-State Pressure Distributions Created by a Well With a Single Infinite-Conductivity Vertical Fracture," *Soc. Pet. Eng. J.* (Aug. 1974) 347-60; *Trans.*, AIME, **257**.
23. Gringarten, A.C., Ramey, H.J. Jr., and Raghavan, R.: "Applied Pressure Analysis for Fractured Wells," *J. Pet. Tech.* (July 1975) 887-92.
24. Bourdet, D. *et al.*: "A New Set of Type Curves Simplifies Well Test Analysis," *World Oil* (May 1983).
25. Bourdet, D. *et al.*: "Interpreting Well Tests in Fractured Reservoirs," *World Oil* (Oct. 1983).
26. Gringarten, A.C. *et al.*: "Evaluating Fissured Formation Geometry From Well Test Data: A Field Example," paper SPE 10182 presented at the 1981 SPE Annual Technical Conference and Exhibition, San Antonio, Oct. 5-7.

Nomenclature

B = formation volume factor
c = fluid compressibility
c_r = rock compressibility
c_t = total compressibility
C = wellbore storage
C_D = dimensionless storage constant
h = formation thickness
k = permeability
ℓ = characteristic length of á matrix block
m = absolute value of semilog straight line slope
n = number of normal sets of fractures
p = pressure
p_D = dimensionless pressure
p_i = initial reservoir pressure
p^* = extrapolated pressure from Horner semi-log straight line
δp = vertical displacement of the two parallel semilog straight lines
Δp = pressure change
q = flow rate
δq = interporosity flow per unit bulk volume per unit time
r = distance to production well
r_w = wellbore radius
S = van Everdingen-Hurst skin factor
s = Laplace transform parameter
t = time
t_D = dimensionless time
t_p = Horner production time
V = ratio of total volume of one porous system to bulk volume
α = block shape parameter
γ = exponential of Euler's constant (=1.78)
λ = interporosity flow coefficient
μ = viscosity
ρ = fluid density
ϕ = porosity of one system
ω = storativity ratio

Subscripts

f = fissure
m = matrix
$f+m$ = total system
t = total
D = dimensionless

SI Metric Conversion Factors

bar	× 1.0*	E+05	=	Pa
bbl	× 1.589 873	E−01	=	m^3
cp	× 1.0*	E−03	=	Pa·s
cu ft	× 2.831 685	E−02	=	m^3
ft	× 3.048	E−01	=	m
in.	× 2.54	E+00	=	cm
md-ft	× 3.008 142	E+02	=	$\mu m^2 \cdot m$
psi	× 6.894 757	E+00	=	kPa

*Conversion factor is exact.

APPENDIX

Double-Porosity Solutions

Warren and Root's solution[2] was derived under the assumption of pseudosteady-state interporosity flow and can be written in the Laplace domain as

$$\bar{p}_D(r_D,s)=\frac{K_0[r_D\sqrt{sf(s)}]}{s\sqrt{sf(s)}\,K_1[\sqrt{sf(s)}]} \quad \ldots\ldots\ldots\ldots (A\text{-}1)$$

for a finite well radius, and as

$$\bar{p}_D(r_D,s)=K_0[r_D\sqrt{sf(s)}] \quad \ldots\ldots\ldots\ldots\ldots\ldots (A\text{-}2)$$

for a line-source well. In Eqs. A-1 and A-2, the Laplace variable is based on the usual dimensionless time based on total reservoir storativity. In engineering units:

$$(t_D)_{f+m}=\frac{0.000264k_f t}{(\phi\mu c_t)_{f+m}\mu r_w^2}. \quad \ldots\ldots\ldots\ldots\ldots\ldots (A\text{-}3)$$

p_D is the dimensionless pressure, given by

$$p_D=\frac{k_f h}{141.2\ qB\mu}\Delta p_f, \quad \ldots\ldots\ldots\ldots\ldots\ldots (A\text{-}4)$$

and r_D, the dimensionless distance to the production well axis:

$$r_D=r/r_w. \quad \ldots\ldots\ldots\ldots\ldots\ldots\ldots\ldots (A\text{-}5)$$

K_0 and K_1 are the modified Bessel functions of the second kind of zero and unit order, respectively. $f(s)$ is introduced by Warren and Root as

$$f(s)=\frac{\omega(1-\omega)s+\lambda}{(1-\omega)s+\lambda}. \quad \ldots\ldots\ldots\ldots\ldots\ldots (A\text{-}6)$$

Using de Swaan's approach,[6] Warren and Root's[2] solution for pseudosteady-state interporosity flow can be extended to transient interporosity flow by simply replacing in Eq. A-1 or A-2 the $f(s)$ function given in Eq. A-6 by[17]

$$f(s)=\omega+\sqrt{\frac{\lambda(1-\omega)}{3s}}\tanh\sqrt{\frac{3(1-\omega)s}{\lambda}}, \quad \ldots\ldots (A\text{-}7)$$

for horizontal slab blocks, and

$$f(s)=\omega+\frac{1}{5}\frac{\lambda}{s}\left[\sqrt{\frac{15(1-\omega)s}{\lambda}}\coth\sqrt{\frac{15(1-\omega)s}{\lambda}}-1\right] \quad \ldots\ldots\ldots\ldots\ldots\ldots (A\text{-}8)$$

for spherical blocks.

In the case of interporosity skin, these become

$$f(s)=\omega+\frac{\sqrt{\frac{\lambda(1-\omega)}{3s}}\tanh\sqrt{\frac{3(1-\omega)s}{\lambda}}}{1+S_{maD}\sqrt{\frac{12(1-\omega)s}{\lambda}}\tanh\sqrt{\frac{3(1-\omega)s}{\lambda}}} \quad \ldots\ldots\ldots\ldots\ldots\ldots (A\text{-}9)$$

for horizontal slab blocks, and

$$f(s)=\omega+\frac{\frac{1}{5}\frac{\lambda}{s}\left[\sqrt{\frac{15(1-\omega)s}{\lambda}}\coth\sqrt{\frac{15(1-\omega)s}{\lambda}}-1\right]}{1+2S_{maD}\left[\sqrt{\frac{15(1-\omega)s}{\lambda}}\coth\sqrt{\frac{15(1-\omega)s}{\lambda}}-1\right]} \quad \ldots\ldots\ldots\ldots\ldots\ldots (A\text{-}10)$$

for spherical blocks, where S_{maD} represents an interporosity skin.*

The effect of skin and wellbore storage on double-porosity behavior was investigated by Mavor and Cinco.[12] Their solution was obtained in the Laplace domain for pseudosteady-state interporosity flow and reads:

$$\bar{p}_D(s)=\frac{K_0[\sqrt{sf(s)}]+S\sqrt{sf(s)}K_1\sqrt{sf(s)}]}{s\left(\sqrt{sf(s)}K_1[\sqrt{sf(s)}]+sC_D\left\{K_0[\sqrt{sf(s)}]+S\sqrt{sf(s)}K_1[\sqrt{sf(s)}]\right\}\right)} \quad \ldots\ldots\ldots\ldots\ldots\ldots (A\text{-}11)$$

with $f(s)$ given by Eq. A-6. C_D is the dimensionless wellbore storage constant, based on total reservoir storativity and given in engineering units by:

$$C_D=(C_D)_{f+m}=\frac{0.8936C}{(\phi Vc_t)_{f+m}hr_w^2}. \quad \ldots\ldots\ldots (A\text{-}12)$$

As before, the corresponding solution for transient interporosity flow is simply obtained by using $f(s)$ from Eqs. A-7, A-8, A-9, or A-10, as appropriate.

*Cinco-Ley, H.: Personal communication (Oct. 28, 1983).

Distinguished Author Series articles are general, descriptive presentations that summarize the state of the art in an area of technology by describing recent developments for readers who are not specialists in the topics discussed. Written by individuals recognized as experts in the areas, these articles provide key references to more definitive work and present specific details only to illustrate the technology. **Purpose:** To inform the general readership of recent advances in various areas of petroleum engineering.